O-Band QPSK modulation based on a silicon dual-drive Mach-Zehnder

Diego Pérez-Galacho[1,2], Laurent Bramerie[3], Charles Baudot[4], Mohamed Chaibi[3,4], Sonia Messaoudène[4], Nathalie Vulliet[4], Laurent Vivien[2], Christophe Peucheret[3] and Delphine Marris-Morini[2]

[1] Universitat Politènica de València, *c/ Camino de Vera s/n – 46022, Valencia - Spain*

Tel: +34963879735, e-mail: diepega@upv.es

[2] *Centre de Nanosciences et de Nanotechnologies, CNRS, Univ. Paris-Sud, Université Paris-Saclay, C2N-Orsay, 91405 Orsay cedex, France*

[3] *Univ Rennes, CNRS, FOTON – UMR 6082, F-22305 Lannion, France*

[4] *STMicroelectronics, 850 rue Jean Monnet, 38920 Crolles, France*

ABSTRACT

Advanced modulation formats will be required in next generation optical interconnects in order to keep up with future bandwidth demand. In this work QPSK modulation in the O-band is experimentally demonstrated using a silicon-based dual-drive Mach-Zehnder modulator.

Keywords: Silicon modulators, silicon photonics, integrated optics, advanced modulation formats, coherent optical communications.

1. INTRODUCTION

Significant research effort has been dedicated over the past years to the development of silicon based photonic technologies. Nowadays, it is believed that silicon photonics is the best suited for next generation short range optical fiber communications [1], [2]. Developing high performance silicon modulators based on the free-carrier plasma dispersion (FCPD) effect [3] has been an important milestone. These modulators are commonly based on carrier depletion in PN junctions and outstanding performances have already been demonstrated [4]–[8]. However, in order to keep up with the growing bandwidth demand in datacom applications, it is necessary to move from binary on-off keying (OOK) modulation formats to more advanced formats such as 4-level pulse amplitude modulation (PAM-4) or quadrature phase-shift keying (QPSK) [9]. Advanced modulation formats using silicon modulators have already been demonstrated [6]–[8]. However, most of these demonstrations have been carried out in the C-band of optical communication systems (1530 nm – 1565 nm) where the FCPD is stronger. Nevertheless, current standards for short range optical fiber communications favour the use of the O-band (1260 nm – 1360 nm) in order to exploit the zero dispersion region of standard single-mode fibers [10]. In this work we present for the first time a QPSK silicon-based dual-drive Mach-Zehnder modulator (DDMZM) operating in the O-band. QPSK generation is normally based on nested MZM structures, therefore requiring four driving signals. However, the QPSK generation based on DDMZM requires only two driving signals, exhibiting a better power efficiency. As first demonstration, 10 GBd (20 Gbps) is shown.

2. MODULATOR DESIGN AND PRINCIPLE OF OPERATION

The cross-section of the designed phase shifter is depicted in Fig. 1(a). It comprises a PN junction implemented in a rib waveguide. It was designed following the simplified modeling approach proposed in [11]. The targeted doping concentrations of the junction were $P = 5 \cdot 10^{17} cm^{-3}$ and $N = 1.4 \cdot 10^{18} cm^{-3}$. The designed phase shifter was integrated in both arms of a Mach-Zehnder interferometer in order to form a DDMZM, schematically represented in Fig. 1(b) in which the Δn_i boxes represent the phase shifting elements and the Φ box symbolizes a fixed phase shift intended to set the operation point of the DDMZM.

In order to generate QPSK modulation using this architecture it is necessary to bias the modulator at the quadrature point ($\Phi = \pi/2$) and to apply the binary in-phase and quadrature-phase modulating signals to each phase shifter so that a phase shift of π can be achieved in each arm [12]. In the designed DDMZM a 1×2 MMI coupler was used as combiner whereas the input splitter was implemented by means of a 2×2 MMI, naturally setting the modulator to the quadrature point. Heaters were introduced in each arm of the DDMZM in order to compensate for fabrication errors and fine tune the bias of the modulator to the quadrature point. GSGSG coplanar traveling wave electrodes were used to apply the two modulating signals to the phase shifters. The active length of the DDMZM was 2 mm. The modulator was fabricated using the 300 mm technological platform from STMicroelectronics [13].

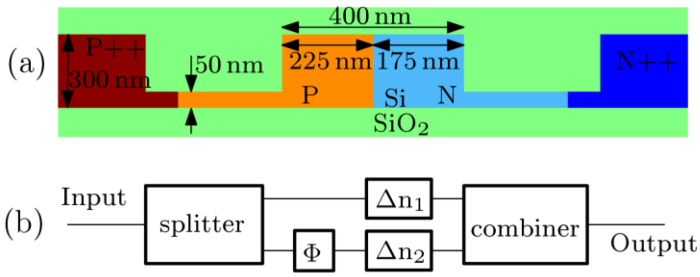

Figure 1. Cross section of the phase shifter (a) and schematic representation of the dual drive Mach-Zehnder modulator (b).

3. CHARACTERIZATION SETUP

In order to assess QPSK modulation, the setup of Fig. 2 was used. TE-polarized light from an O-band external laser was injected in/out of the fabricated chip using grating couplers. RF and DC electrical probes were used to electrically drive the phase shifters and heaters, respectively. Two 2^{15}-1 long de-correlated pseudo random binary sequence (PRBSs) at 10 Gbps were used as modulating signals. The two PRBSs modulating signal were amplified and then a DC bias was added to ensure that the PN junctions were operated in depletion. The driving signals applied to the phase-shifters had peak-to-peak voltages of $7V_{pp}$ with a DC bias of 4V. 50Ω loads were added at the end of the GSGSG coplanar electrodes. The signal at the output of the modulator was then input to an integrated coherent receiver through a variable optical attenuator in order to control the received power. For the purpose of this first demonstration, the same laser was used as local oscillator in the receiver, therefore implementing an homodyne detection scheme. The I/Q output signals of the receiver were fed to a 40 Gsps digital sampling oscilloscope. 10^5 symbols were acquired and then processed offline. For digital processing, an adaptive finite impulse response (FIR) filter with decision-directed least mean square (DD-LMS) tracking was used.

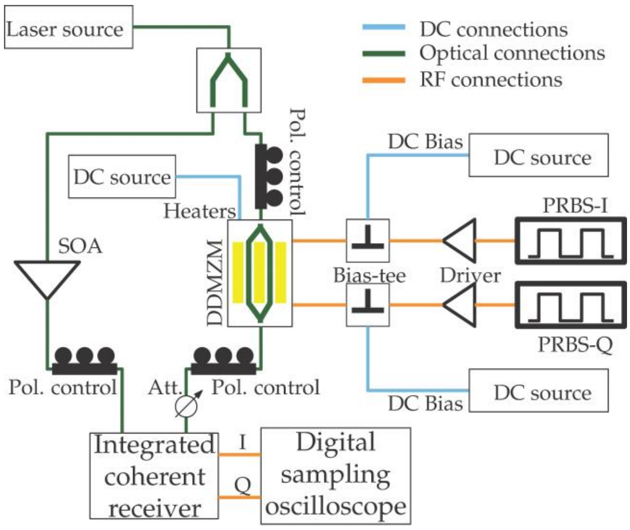

Figure 2. Experimental setup employed for QPSK signal characterization.

4. CHARACTERIZATION SETUP

The DDMZM was first characterized in DC. The measured fiber-to-fiber attenuation was 17 dB, including the loss of the grating couplers, on-chip passive losses and modulator insertion loss (IL). Using a straight waveguide on the chip as normalization, the IL of the modulator was estimated to be 3.8 dB. The V_π of each phase shifter was measured to be between 6 V and 7 V. Taking into account the 2 mm active length, this leads to a modulation efficiency between 1.2 V·cm and 1.4 V·cm.

High-speed measurements were then performed on the modulator. Using the setup previously described, the bit error rate (BER) was measured as a function of the signal average received power, as shown in Fig. 3(a). Each point in the BER curve of Fig. 3(a) is the result of the averaging of five BER measurements, each carried out on 10^5 transmitted symbols. Using a BER value of 10^{-3} as the limit for error free transmission based on forward error correction, the required received power is of -20dBm. The received constellation diagram after offline digital signal processing is shown in Fig. 3(b) for a received power of -22 dBm. A clear QPSK constellation diagram can be seen, and the measured EVM for this constellation is 33%.

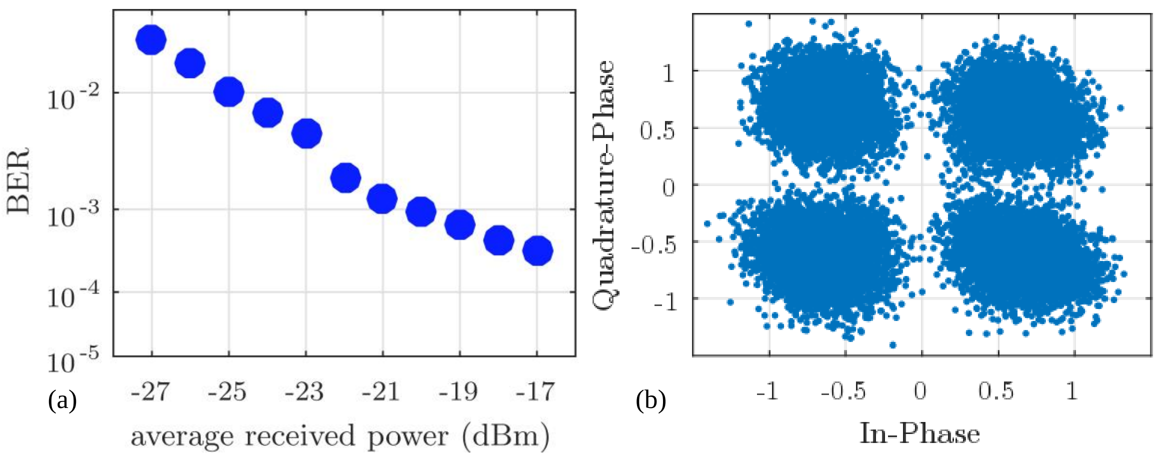

Figure 3 BER as a function of the received power (a) and measured constellation diagram for a received power of -22dBm (b).

5. CONCLUSIONS

Short range optical communication systems in the O-Band are facing important demands of bandwidth nowadays. As a first step towards more efficient modulation schemes, QPSK modulation in the O-band using a silicon modulator has been proposed and experimentally demonstrated at 10GBd (20GBps) for the first time using a DDMZM. The benefit of this modulator is that, relying on a single Mach-Zehnder interferometer, it only requires two driving signals, whereas standard QPSK modulation based on nested MZMs require four driving signals. This reduction on power consumption will be an important advantage in framework of short range communications.

ACKNOWLEDGEMENTS

This work was supported by the European projects Plat4m (FP7-2012-318178), Cosmicc (H2020-ICT-27-2015-688516). We acknowledge the support of French Industry Ministry/DGE through the Nano2017 program.

REFERENCES

[1] B. Jalali and S. Fathpour: Silicon photonics, *J. Lightw. Technol.*, vol. 24, no. 12, pp. 4600–4615, 2006.
[2] M. J. Paniccia: A perfect marriage: optics and silicon, *Optik & Photonik*, vol. 6, no. 2, pp. 34–38, 2011.
[3] R. A. Soref and B. R. Bennett: Electrooptical effects in silicon, *IEEE J. Quantum Electron*., vol. 23, no. 1, pp. 123–129, 1987.
[4] D. Perez-Galacho *et al.*: Low voltage 25Gbps silicon Mach-Zehnder modulator in the O-band, *Opt. Express* 25, 11217-11222 (2017)
[5] D. J. Thomson *et al.*: Silicon carrier depletion modulator with 10 Gbit/s driver realized in high-performance photonic biCMOS, *Laser & Photonics Reviews*, vol. 8, no. 1, pp. 180–187, 2014.
[6] J. Wang *et al.*: Silicon high-speed binary phase-shift keying modulator with a single-drive push–pull high-speed traveling wave electrode, *Photon. Res.*, vol. 3, no. 3, pp. 58–62, 2015.
[7] P. Dong *et al.*: Silicon in-phase/quadrature modulator with on-chip optical equalizer, *J. Lightw. Technol.*, vol. 33, no. 6, pp. 1191–1196, 2015.
[8] Q. Li *et al.*: High-speed BPSK modulation in silicon, *IEEE Photon. Technol. Lett.*, vol. 27, no. 12, pp. 1329–1332, 2015.
[9] A. Shacham *et al.*: Photonic networks-on-chip for future generations of chip multiprocessors, *IEEE Trans. Comput.*, vol. 57, no. 9, pp. 1246–1260, 2008.
[10] Physical Layer Specifications and Management Parameters for 40 Gb/s and 100 Gb/s Operation over Fiber Optic Cables, IEEE Standard for Ethernet Std.
[11] D. Perez-Galacho *et al.*: Simplified modeling and optimization of silicon modulators based on free-carrier plasma dispersion effect, *Opt. Express*, vol. 24, no. 23, pp. 26 332–26 337, Nov 2016.
[12] K.-P. Ho and H.-W Cuei: Generation of arbitrary quadrature signals using one dual-drive modulator, *J. Lightw. Technol.*, vol. 23, no. 2, pp. 764–770, 2006.
[13] C. Baudot *et al.*: DAPHNE silicon photonics technological platform for research and development on WDM applications, *in SPIE Photonics Europe*. 2016, pp. 98 911D–98 911D.